Journal of Science and Engineering Technology, Vol. 5, No. 3, pp. 13-20 (2009)

A Nanostructural Zinc Oxide Electrode Prepared by a Hydrothermal Method for Dye-Sensitized Solar-Cell Application

SHIH-FONG LEE, LI-YING LEE and YUNG-PING CHANG
Department of Electrical Engineering, Da-Yeh University
No. 168, University Rd., Dacun, Changhua, Taiwan 51591, R.O.C.

ABSTRACT

In this study, zinc oxide (ZnO) nanorods were synthesized on indium-tin-oxide (ITO) glass substrates by a hydrothermal process using various molar concentrations of $Zn(NO_3)_2 \cdot 6H_2O + C_6H_{12}N_4$. Subsequently, scanning electron microscopy (SEM), energy dispersive spectroscopy (EDS), and x-ray diffraction (XRD) were used to obtain the surface morphology, chemical composition, and crystallographic structure of the nanorods. These nanorods were then submerged in a dye solution and used as the working electrode for a dye-sensitized solar cell (DSSC). The *I-V* and optoelectronic characteristics of DSSCs using the nanorods prepared by various concentrations of $Zn(NO_3)_2 \cdot 6H_2O + C_6H_{12}N_4$ as the electrodes were measured to obtain their fill factors and conversion efficiency. The experimental results revealed that the ZnO film prepared by 0.2M of this compound exhibits a uniform distribution of dense nanorods whose shape and microstructure are beneficial to dye adsorption and carrier transport. Therefore, the DSSC fabricated with the nanorods prepared by the 0.2M process has an improved short-circuit current, fill factor, and conversion efficiency.

Key Words: zinc oxide (ZnO) nanorods, dye-sensitized solar cell (DSSC)

以水熱法製備氧化鋅奈米結構電極應用於染敏太陽能電池之研究

李世鴻　李麗英　張永平
大葉大學電機工程學系
51591 彰化縣大村鄉學府路 168 號

摘　要

在本實驗中，我們先使用水熱法在銦錫氧化物（indium-tin-oxide, ITO）玻璃基板上成長氧化鋅（ZnO）奈米柱。成長過程使用不同莫爾濃度的硝酸鋅六水合物（zinc nitrate hexahydrate, $Zn(NO_3)_2 \cdot 6H_2O$）及六亞甲基四胺（hexamethylenetetramine, $C_6H_{12}N_4$）混合溶液以得到 ZnO 奈米柱。此外，我們也把成長完成的 ZnO 奈米柱浸泡在染料中製作成染敏太陽能電池

（dye-sensitized solar cell, DSSC）元件。我們利用掃描式電子顯微鏡（scanning electron microscopy, SEM）、能量散佈能譜（energy dispersive spectroscopy, EDS）及 X 光繞射儀（x-ray diffraction, XRD）等量測分析對不同莫爾濃度混合溶液所成長的 ZnO 奈米柱的表面型態、化學成分與晶格結構，並對使用不同莫爾濃度混合溶液所成長的 ZnO 奈米柱作爲工作電極所製作而成的 DSSC 進行 I-V 電性及照光特性分析。由實驗結果得知，0.2M 的 $Zn(NO_3)_2$•$6H_2O$+$C_6H_{12}N_4$ 所成長的 ZnO 奈米柱可以增加工作電極的緻密度及均勻性，其幾何形狀、表面分佈及微結構等特性可以增加染料的吸附數量，並且有利於載子的傳輸。因此，使用 0.2M 的 $Zn(NO_3)_2$•$6H_2O$+$C_6H_{12}N_4$ 所成長的 ZnO 奈米柱來製作的 DSSC 可得到改善的短路電流、填充因子及轉換效率。

關鍵詞：氧化鋅奈米柱，染敏太陽能電池

I. INTRODUCTION

Zinc oxide (ZnO) is a wide-bandgap II-VI compound semiconductor with a direct bandgap of 3.37 eV at room temperature. With an electron binding energy of 60 meV [22] and the superior properties such as anti-oxidation and chemical stability, ZnO is a promising optoelectronic material with great potential in applications for optical detector [13], gas sensor [6], solar cell [10], short-wavelength UV laser, and blue or green optoelectronic devices [2]. In the present time, the synthesis of ZnO with novel shapes (e.g. wire, rod, lamina, and tube) has attracted widespread attention.

Many processes have been used to prepare ZnO including thermal evaporation [11, 15], pulsed laser deposition (PLD) [4], magnetic enhanced sputter [12], metal-organic chemical vapor deposition (MOCVD) [16], and chemical vapor deposition [23]. However, the processes stated above not only require expensive equipment but also are not suitable for batch-type production. In comparison, using chemical solution to prepare ZnO has several advantages over the processes stated above. Not only it is an inexpensive process with low-cost equipment, but also ZnO with excellent crystallinity, chemical stability, and thermal stability can be attained with this process. The relative merit of using hydrothermally grown nanorods in DSSC application has been thoroughly studied by Hsu [7].

ZnO was used to fabricate electrode much earlier than TiO_2. Early in 1969, Gerischer et al. [5] studied the feasibility of using crystalline ZnO electrode in dye-sensitized solar cell (DSSC); Tsubomura and coworkers [19] presented a report on the research of the optoelectronic characteristics of DSSC with ZnO electrode in 1976; Matsumura and coworkers [14] used porous ZnO as the electrode to achieve a conversion efficiency of 2.5% at the wavelength of 562 nm in 1980. In 1994, Redmond et al. [17] used ruthenium as the dye to obtain a monochromatic conversion efficiency of 13% at the wavelength of 520 nm and a conversion efficiency of 0.4% under sunlight. In 1997, Rensmo et al. [18] reported a monochromatic conversion efficiency as high as 58% and a conversion efficiency of 2% under sunlight. These results clearly demonstrated the plausibility of using ZnO in the high efficiency DSSC. In the study by Keis and coworkers [9] in 2002, the conversion efficiency of ZnO solar cell under direct sunlight (100 W/m^2) was 5%. And the highest conversion efficiency reported by Kakiuchi and coworkers [8] for ZnO solar cell under full sunlight (AM-1.5, 100 mW/cm^2) is 4.1%.

The incorporation of crystalline semiconductor nanowires can effectively lower the potential barrier at the grain boundary and reduce the loss of electron transport. Therefore, transport property of carrier is improved and the conversion efficiency of solar cell is increased [1]. Hence, they have become the material selection for electrode in DSSC device application. In this study, ZnO nanorods were synthesized with an inexpensive hydrothermal process. The purpose of using ZnO nanorods as the working electrode (anode) in a DSSC was to increase its carrier transport capability. ZnO nanorods were used with the intention to increase the adsorption of dye thereby increasing the optical absorption and rendering higher conversion efficiency for the DSSC. The *I-V* characteristics of DSSCs using ZnO nanorods prepared by various molar concentrations of $Zn(NO_3)_2$•$6H_2O$+$C_6H_{12}N_4$ as the working electrode (anode) were measured and investigated to study their effects on the conversion efficiency of solar cell.

II. EXPERIMENTAL DETAILS

In this work, ZnO nanorods prepared by a simple hydrothermal process were used to fabricate the working electrodes (anodes) for DSSC applications. First, an indium-tin-oxide (ITO) glass substrate was cut into 2cm × 2cm pieces, and then rinsed with acetone, methanol and deionized

water. After cleaning, the ITO glass substrates were blown with nitrogen to dry. Transparent tapes were adhered along the peripheral of ITO glass substrate. Thus, only the central area of 1cm × 1cm was reserved for the growth for ZnO nanorods. In addition to ITO substrates, ZnO nanorods were also synthesized on silicon substrates since they are more suitable for SEM and EDS measurements. Second, deionized water was added to zinc nitrate hexahydrate ($Zn(NO_3)_2$•$6H_2O$) and hexamethylenetetramine ($C_6H_{12}N_4$, HMT) to obtain the reagents for the growth of ZnO nanorods. These two solutions were mixed at the ratio of 1:1. The mixed solution was vigorously stirred for 20 minutes at room temperature to ensure full and uniform mixing. The mixture was heated indirectly through water at 80-85ºC. After the temperature of mixture was stabilized, ITO glass substrates were submerged in the mixture with ITO facing upwards. After 1 hour of high temperature process, samples were removed from the beaker and were rinsed with deionized water for 20 minutes to halt the growth process of ZnO nanorods. Finally, the synthesized ZnO samples were placed into a box for 5 hours so that they can dry naturally. After the working electrodes using ZnO nanorods prepared by various concentrations of $Zn(NO_3)_2$•$6H_2O$+$C_6H_{12}N_4$ were fabricated, they were submerged in dye solution for 8 hours so that dyes can be fully adsorbed by ZnO nanorods. Subsequently, the working electrodes were assembled with the counter electrode of Pt film/ITO glass and electrolyte was injected to form the DSSC.

The purpose of this work is to study the surface morphology, chemical composition, and microstructure of the ZnO nanorods prepared by various molar concentrations of $Zn(NO_3)_2$•$6H_2O$+$C_6H_{12}N_4$. Scanning electron microscopy (SEM), energy dispersive spectrometry (EDS), and x-ray diffraction (XRD) were used to obtain the surface morphology, chemical composition, and crystallographic structure of ZnO nanorods. Afterwards, *I-V* characteristics of the DSSCs using ZnO nanorods prepared by various molar concentrations of $Zn(NO_3)_2$•$6H_2O$+$C_6H_{12}N_4$ were measured, and their open-circuit voltage, short-circuit current, fill factor, and conversion efficiency were determined.

III. RESULTS AND DISCUSSION

In this study, ZnO were prepared with zinc nitrate hexahydrate ($Zn(NO_3)_2$•$6H_2O$) and hexamethylenetetramine ($C_6H_{12}N_4$, HMT) in a hydrothermal process. These two reagents were mixed at the ratio 1:1 in water. The molar concentration ratio of $Zn(NO_3)_2$•$6H_2O$ and $C_6H_{12}N_4$ was 1:1 as proposed by Vayssieres [20]. HMT is non-toxic and its water-soluble polymer ring dissolves in the acidic solution into functional groups to form NH_3. $Zn(NO_3)_2$ can react with HMT in water to synthesize ZnO nanorods. The chemical reactions involved in the growth of ZnO nanorods are: [3, 21, 24]

$$C_6H_{12}N_4 + 6H_2O \rightarrow 6HCHO + 4NH_3 \quad (1)$$

$$NH_3 + H_2O \rightarrow NH_4^+ + OH^- \quad (2)$$

$$2OH^- + Zn^{2+} \rightarrow ZnO + H_2O \quad (3)$$

First, $C_6H_{12}N_4$ was disintegrated into formaldehyde (HCHO) and ammonia (NH_3) as shown in equation (1). Ammonia tends to disintegrate water to produce OH^- anions (equation 2). Finally, OH^- anions react with Zn^{2+} cations to synthesize ZnO (equation 3). In the growth process of ZnO nanorods, the concentration of OH^- anions is the dominant factor. Therefore, $C_6H_{12}N_4$ that supplies OH^- anions plays a key role in the growth of ZnO nanorods. The hydrolysis rate of $C_6H_{12}N_4$ is low and thus can provide OH^- anions at a steady rate rendering a solution with a constant concentration of OH^- anions. At low concentrations of $C_6H_{12}N_4$ and $Zn(NO_3)_2$•$6H_2O$, the reaction rate of OH^- anions is low; on the other hand, at high concentrations of $C_6H_{12}N_4$ and $Zn(NO_3)_2$•$6H_2O$, the chemical reaction rate and the growth rate of ZnO nanorods is high. In this study, the molar concentration of mixture was varied to study its effect on the surface morphology, chemical composition, and optoelectronic properties of the synthesized ZnO nanorods.

Figure 1 shows the top-view SEM images of the ZnO nanorods prepared by various concentrations of $Zn(NO_3)_2$•$6H_2O$+$C_6H_{12}N_4$. The enlarged images are shown in Figure 2. The magnification is 1×10^3 for Figure 1 and is 3×10^4 for Figure 2. The growth parameters are listed as follows: the growth temperature was 80-85ºC, growth time was 1 hour, and the molar concentrations of $Zn(NO_3)_2$•$6H_2O$+$C_6H_{12}N_4$ were 0.025M, 0.05M, 0.1M, 0.2M and 0.3M. In Figure 1(a), ZnO nanorods are distributed sparsely on the substrate and the underlying substrate can be clearly seen. For ZnO nanorods prepared with 0.05M $Zn(NO_3)_2$•$6H_2O$+$C_6H_{12}N_4$, the surface density of ZnO nanorods become higher, but a portion of the substrate still exposes. The substrate is completely covered by ZnO nanorods as the molar concentration of $Zn(NO_3)_2$•$6H_2O$+$C_6H_{12}N_4$ is increased to 0.1M or higher as seen in Figures 1(c), (d), and (e). The average diameters (distance between any two parallel sidewalls) of ZnO nanorods prepared by various concentrations of $Zn(NO_3)_2$•$6H_2O$+$C_6H_{12}N_4$ are shown in Figure 3. The average diameter of nanorods increases linearly from ~385 nm for the

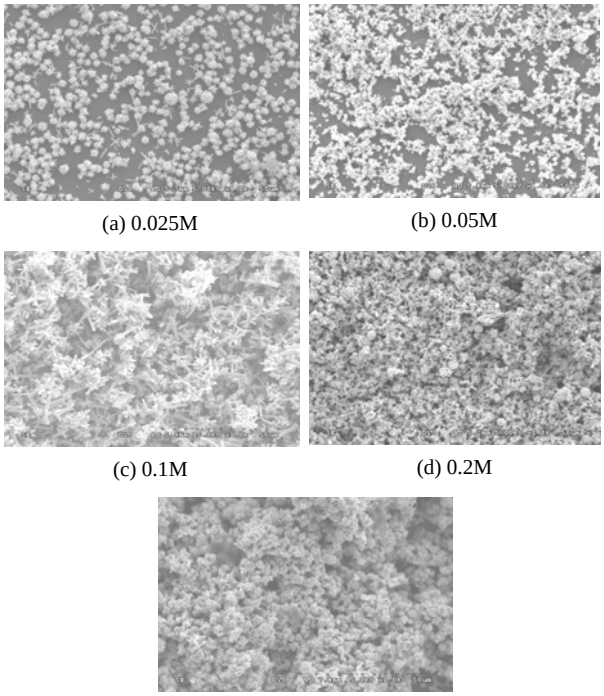

(a) 0.025M (b) 0.05M

(c) 0.1M (d) 0.2M

(e) 0.3M

Fig. 1. The top-view SEM images of ZnO nanorods prepared by various concentrations of $Zn(NO_3)_2$•$6H_2O$+$C_6H_{12}N_4$. The magnification factor is 1×10^3.

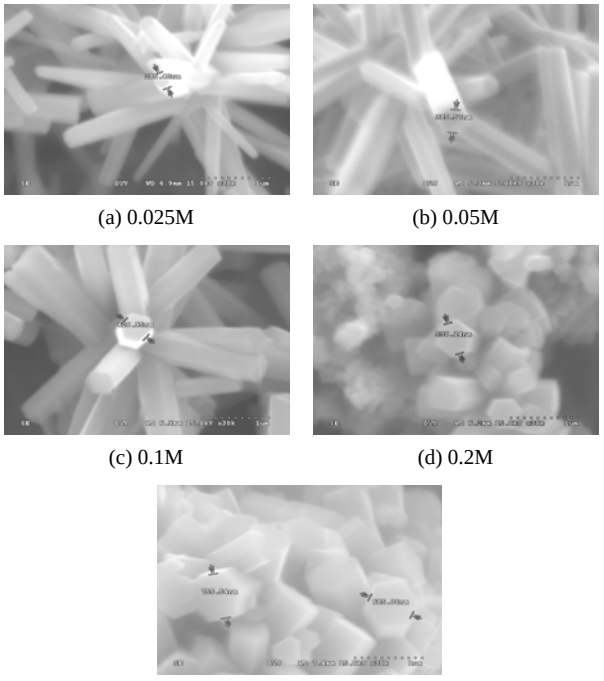

(a) 0.025M (b) 0.05M

(c) 0.1M (d) 0.2M

(e) 0.3M

Fig. 2. The enlarged top-view SEM images of ZnO nanorods prepared by various concentrations of $Zn(NO_3)_2$•$6H_2O$+$C_6H_{12}N_4$. The magnification factor is 3×10^4.

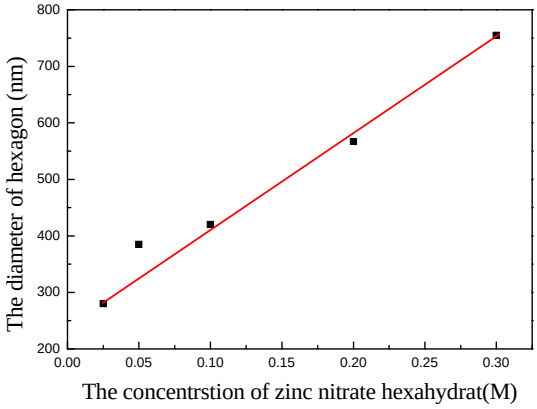

Fig. 3. Average diameter of ZnO nanorods prepared by various concentrations of $Zn(NO_3)_2$•$6H_2O$ +$C_6H_{12}N_4$.

ZnO nanorods prepared by 0.025M of $Zn(NO_3)_2$•$6H_2O$+$C_6H_{12}N_4$ to ~755 nm for the ZnO prepared by 0.3M of $Zn(NO_3)_2$•$6H_2O$+$C_6H_{12}N_4$.

It is worth noting that the diameter near the tip of hexagonal pillar may not be the same as that near the bottom. As seen in Figure 2(a), the diameter near the tip of hexagonal pillar is smaller than that near the bottom for the ZnO nanorods prepared by 0.025M of $Zn(NO_3)_2$•$6H_2O$+$C_6H_{12}N_4$. In contrast, the diameters near the tip and the bottom of hexagonal pillar are almost the same for the ZnO nanorods prepared with 0.05M and 0.1M of $Zn(NO_3)_2$•$6H_2O$+$C_6H_{12}N_4$. As the molar concentration of $Zn(NO_3)_2$•$6H_2O$+$C_6H_{12}N_4$ is increased to 0.2M and 0.3M, the synthesized ZnO nanorods become short and wide. Therefore, it can be deduced that the increase in the growth rate on the six sidewalls is higher than that on the tip surface. And it is reasonable for the shape of ZnO nanorods to become short and wide as the molar concentration of $Zn(NO_3)_2$•$6H_2O$+$C_6H_{12}N_4$ is increased. Since the surfaces of ZnO nanorods films are rough, their thickness can only be estimated from the side-view SEM images (not shown here). Figure 4 shows the relationship between the estimated film thickness of ZnO nanorods and the molar concentration of $Zn(NO_3)_2$•$6H_2O$+$C_6H_{12}N_4$ used in the growth process. A linear relationship is obtain between the film thickness of ZnO nanorod film and the molar concentration of $Zn(NO_3)_2$•$6H_2O$+$C_6H_{12}N_4$.

In this study, EDS was used to measure the chemical composition of ZnO nanorods prepared by various molar concentrations of $Zn(NO_3)_2$•$6H_2O$+$C_6H_{12}N_4$ which is listed in Table 1. As observed in the EDS analysis, the atomic content of silicon in the ZnO nanorods prepared by 0.025M of $Zn(NO_3)_2$•$6H_2O$+$C_6H_{12}N_4$ is 32.82%. Since no

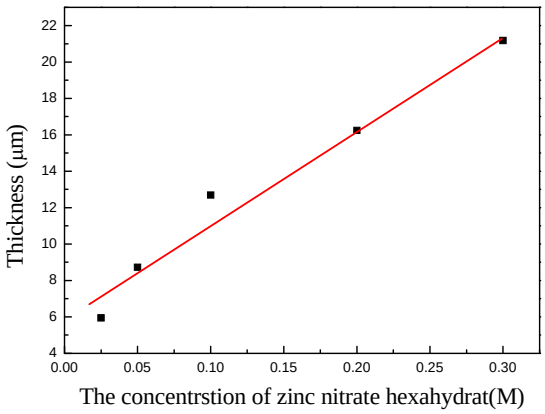

Fig. 4. Film thickness of ZnO nanorods prepared by various concentrations of $Zn(NO_3)_2$•$6H_2O$+$C_6H_{12}N_4$.

Table 1. Chemical composition for the ZnO nanorods prepared by various molar concentrations of $Zn(NO_3)_2$•$6H_2O$+$C_6H_{12}N_4$

	Atomic percentage (%)				
	0.025M	0.05M	0.1M	0.2M	0.3M
O	60.63	72.03	77.82	74.35	61.95
Si	32.82	17.26	2.80	0.00	0.00
Zn	6.55	10.71	19.37	25.65	38.05
Zn:O	1:9.26	1:6.73	1:4.02	1:2.90	1:1.62

silicon-containing reagent was used in the growth process, the detected silicon content is caused by silicon atoms on the substrate. Obviously, the ZnO nanorods are not dense enough to completely cover the entire substrate and a portion of the substrate is exposed. The atomic percentage of silicon drops to17.26% and 2.8% as the concentration of $Zn(NO_3)_2$•$6H_2O$+$C_6H_{12}N_4$ is increased to 0.05M and 0.1M. This is a clear indication that more ZnO nanorods were synthesized on the substrate and their distribution become more uniform and denser. As the concentration of $Zn(NO_3)_2$•$6H_2O$+$C_6H_{12}N_4$ is further increased to 0.2M and 0.3M, the atomic percentage drops to zero indicating that substrate is completely covered by ZnO nanorods. These results are consistent with those obtained from SEM images as shown in Figure 1. This is beneficial to the uniform adsorption of dye molecules.

The chemical composition for ZnO nanorods prepared by various concentrations of $Zn(NO_3)_2$•$6H_2O$+$C_6H_{12}N_4$ can be clearly seen in Table 1. The atomic ratio of zinc to oxygen decreases with the increasing concentration of $Zn(NO_3)_2$•$6H_2O$+$C_6H_{12}N_4$. The atomic ratio of zinc to oxygen on the surface of nanorods is 1:9.26 for ZnO nanorods prepared by 0.025M of $Zn(NO_3)_2$•$6H_2O$+$C_6H_{12}N_4$. Whereas this atomic ratio decreased to 1:1.62 for ZnO nanorods prepared by 0.3M of $Zn(NO_3)_2$•$6H_2O$+$C_6H_{12}N_4$ which is close to the theoretical value of 1 as is expected for ZnO.

Figure 5 shows the XRD spectra for the ZnO nanorods prepared by various molar concentrations of $Zn(NO_3)_2$•$6H_2O$+$C_6H_{12}N_4$. All spectra exhibit five characteristic peaks. The diffraction peaks located at diffraction angles of 2θ = 31.77°, 34.42° and 36.25° are more pronounced. These 3 peaks correspond to (100), (002) and (101) directions of crystallization of wurtzite ZnO nanorods, i.e., the growth along the directions of *a*, *b*, and *c*-axis of nanorod hexagonal structure, respectively. Also found in the diffraction spectra are two additional smaller characteristic peaks corresponding to (102) and (110) directions, respectively, indicating the polycrystalline structure of ZnO nanorods.

Intensities of characteristic peaks in XRD spectra for the ZnO nanorods prepared by various molar concentrations of $Zn(NO_3)_2$•$6H_2O$+$C_6H_{12}N_4$ are listed in Table 2. In the diffraction spectra, the intensity ratio in the direction of *a* axis and *c* axis (I_a/I_c) and the intensity ratio in the direction of *a* axis and *c* axis (I_b/I_c) are useful. The values of I_a/I_c and I_b/I_c increase with the molar concentration of $Zn(NO_3)_2$•$6H_2O$+$C_6H_{12}N_4$. The value of I_a/I_c increases 1.18 to 1.47, and I_b/I_c increases from 1.74 to 2.02. The aspect ratio of nanorod also increases with the molar concentration of $Zn(NO_3)_2$•$6H_2O$+$C_6H_{12}N_4$ used in the growth process. At low concentrations of $Zn(NO_3)_2$•$6H_2O$+$C_6H_{12}N_4$, the growth rate on the (002) surface is the fast and hence is the preferential direction for growth. However, at 0.2M of $Zn(NO_3)_2$•$6H_2O$+$C_6H_{12}N_4$, the increase in the growth rate on the (100) and (101) surfaces of ZnO nanorods are higher than that on the (002) surface. Hence, ZnO nanorods become short and wide at high concentrations of $Zn(NO_3)_2$•$6H_2O$+$C_6H_{12}N_4$ as can be verified by the SEM image shown in Figure 1(d) and (e).

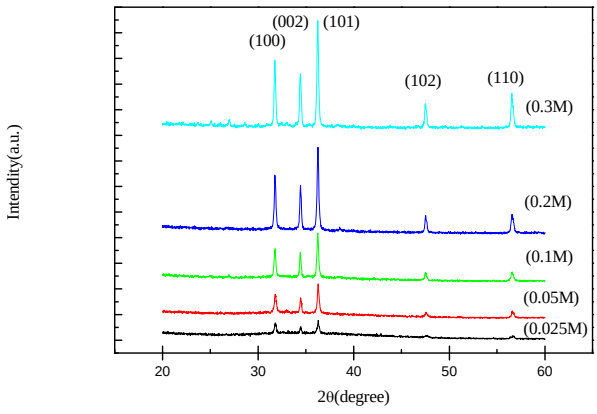

Fig. 5. XRD spectra for the ZnO nanorods prepared by various concentrations of $Zn(NO_3)_2$•$6H_2O$+$C_6H_{12}N_4$.

Table 2. Intensities of characteristic peaks in XRD spectra for the ZnO nanorods prepared by various molar concentrations of $Zn(NO_3)_2$•$6H_2O$+$C_6H_{12}N_4$

	a axis	*c* axis	*b* axis	I_a/I_c	I_b/I_c
0.025M	391	266	384	1.09	1.44
0.05M	440	389	630	1.13	1.62
0.1M	602	511	893	1.18	1.74
0.2M	1058	856	1413	1.23	1.88
0.3M	1270	1015	2055	1.25	2.02

Figure 6 shows the *J-V* characteristics of the DSSCs fabricated with ZnO nanorods prepared by various molar concentrations of $Zn(NO_3)_2$•$6H_2O$+$C_6H_{12}N_4$. Their open-circuit voltage (V_{oc}), short-circuit current (I_{sc}), and fill-factor (FF) are tabulated in Table 3. For the DSSCs fabricated with ZnO nanorods prepared by 0.025M and 0.05M of $Zn(NO_3)_2$•$6H_2O$+$C_6H_{12}N_4$, short-circuit current and fill factor are very low. In sharp contrast, the DSSCs fabricated with ZnO nanorods prepared by 0.2M and 0.3M of $Zn(NO_3)_2$•$6H_2O$+$C_6H_{12}N_4$ exhibits much improved short-circuit current and fill factor, and hence a much higher conversion efficiency.

For the ZnO nanorods prepared by 0.025M and 0.05M of

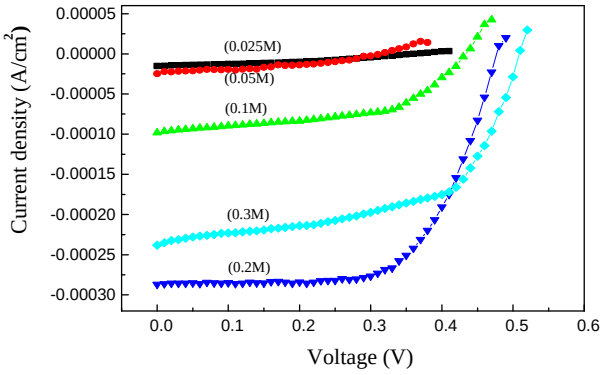

Fig. 6. *J-V* characteristics of the DSSCs using ZnO nanorods prepared by various concentrations of $Zn(NO_3)_2$•$6H_2O$+$C_6H_{12}N_4$ as the working electrode.

Table 3. Open-circuit voltage (V_{oc}), short-circuit current (I_{sc}), and fill factor (FF) for the DSSCs using ZnO nanorods prepared by various molar concentrations of $Zn(NO_3)_2$•$6H_2O$+$C_6H_{12}N_4$

	V_{oc} (V)	I_{sc} (A)	FF (%)
0.025M	0.32	1.537×10^{-5}	33.217
0.05M	0.37	2.491×10^{-5}	35.546
0.1M	0.44	9.812×10^{-5}	53.101
0.2M	0.48	2.869×10^{-4}	63.862
0.3M	0.51	2.382×10^{-4}	57.989

$Zn(NO_3)_2$•$6H_2O$+$C_6H_{12}N_4$, the distribution of nanorods on the ITO glass substrate is sparse and non-uniform. Lots of voids and vacancies are found in the ZnO film so that dye molecules can not uniformly adsorbed in the film. Therefore, the DSSC fabricated with the ZnO nanorods prepared by 0.025M and 0.05M molar concentrations of $Zn(NO_3)_2$•$6H_2O$+$C_6H_{12}N_4$ exhibit poor *I-V* characteristics. The distribution of ZnO nanorods prepared by 0.1M of $Zn(NO_3)_2$•$6H_2O$+$C_6H_{12}N_4$ is still non-uniform indicating that there are still some voids and vacancies in the ZnO film. This can affect the adsorption of dye molecules so that only slight improvement in the *I-V* characteristics of DSSC can be achieved. For the DSSCs using ZnO nanorods prepared by 0.2M and 0.3M molar concentrations of $Zn(NO_3)_2$•$6H_2O$+$C_6H_{12}N_4$, improvement in their *I-V* characteristics can be clearly seen. Compared with the DSSC fabricated with ZnO nanorods prepared by 0.025M of $Zn(NO_3)_2$•$6H_2O$+$C_6H_{12}N_4$, short-circuit current increases by more than one order of magnitude, fill factor also increase, and a large increase in conversion efficiency is achieved. From the atomic ratio of zinc to oxygen in EDS analysis, the structure of the ZnO nanorods prepared by 0.2M and 0.3M of $Zn(NO_3)_2$•$6H_2O$+$C_6H_{12}N_4$ is much better than that of the ZnO nanorods prepared by 0.025M of $Zn(NO_3)_2$•$6H_2O$+$C_6H_{12}N_4$. Much fewer voids or bonding vacancies are present in the nanorods. Therefore, electrons are easier to travel in these films and the conversion efficiency of DSSC is increased.

However, the *I-V* characteristics for the DSSC fabricated with ZnO nanorods prepared by 0.3M of $Zn(NO_3)_2$•$6H_2O$+$C_6H_{12}N_4$ are inferior to those of the DSSC prepared with ZnO nanorods prepared by 0.2M. Short-circuit current and fill factor are lower, and hence a lower conversion efficiency is achieved. The reason for the degradation in the *I-V* characteristics as found in the DSSC prepared with ZnO nanorods prepared by 0.3M of $Zn(NO_3)_2$•$6H_2O$+$C_6H_{12}N_4$ is presumably caused by the larger thickness of ZnO film. The distance that electrons have to travel through the ZnO film is increased, and electron-hole recombination is more likely to take place. Hence, photocurrent is decreased accordingly. Besides, the average diameter of ZnO nanorods becomes larger for the ZnO nanorods prepared by 0.3M molar concentration of $Zn(NO_3)_2$•$6H_2O$+$C_6H_{12}N_4$ so that the aspect ratio of nanorods increases and nanorod become short and wide. The voids and vacancies lying between nanorods become larger, and an intimate contact between nanorods is unlikely now. This results in an increase in the internal resistance of working electrode. Fill factor and conversion efficiency are decreased drastically and the operating characteristics of DSSC are severely degraded.

IV. CONCLUSIONS

In this study, ZnO nanorods prepared by various molar concentrations of $Zn(NO_3)_2 \cdot 6H_2O + C_6H_{12}N_4$ were used as the working electrodes for DSSCs. Experimental results reveal that the average diameter of ZnO nanorods increases with the molar concentration of $Zn(NO_3)_2 \cdot 6H_2O + C_6H_{12}N_4$. As the concentration of $Zn(NO_3)_2 \cdot 6H_2O + C_6H_{12}N_4$ is increased, the shape of the synthesized ZnO nanorods varies from long, slender hexagonal pillars to short, wide rods. As the concentration of $Zn(NO_3)_2 \cdot 6H_2O + C_6H_{12}N_4$ is increased to 0.2M, substantial improvement in the open-circuit voltage, short-circuit current, and conversion efficiency of DSSC are achieved. However, as the molar concentration of $Zn(NO_3)_2 \cdot 6H_2O + C_6H_{12}N_4$ is further increased to 0.3M, the average diameter of nanorods increases to lower the specific surface area. Less dye molecules are adsorbed which make the photocurrent decrease. Another possible factor is the increase of internal resistance in the ZnO nanorod working electrode which can lower fill factor and conversion efficiency.

REFERENCES

1. Baxter, J. B. and E. S. Aydil (2005) Dye-sensitized solar cells based on semiconductor morphologies with ZnO nanowires. *Solar Energy Materials and Solar Cells*, 90(5), 607-622.
2. Cao, H., J. Y. Xu, E. W. Seelig and R. P. H. Chang (2000) Microlaser made of disordered media. *Applied Physics Letters*, 76, 2997-2999.
3. Chen, Z. and L. Gao (2006) A facile route to ZnO nanorod arrays using wet chemical method. *Journal of Crystal Growth*, 293, 522-527.
4. Choi, J. H., H. Tabata and T. Kawai (2001) Initial preferred growth in zinc oxide thin films on Si and amorphous substrates by a pulsed laser deposition. *Journal of Crystal Growth*, 226, 493-500.
5. Gerischer, H., H. Tributsch and B. Bunsenger (1969) Elektrochemische Untersuchungen über den Mechanismus der Sensibilisierung und Übersensibilisierung an ZnO-Einkristallen. *Physical Chemistry*, 73(1), 251-260.
6. Golego, N., S. A. Studenikin and M. Cocivera (2000) Sensor photoresponse of thin-film oxides of zinc and titanium to oxygen gas. *Journal of the Electrochemical Society*, 147, 1592-1594.
7. Hsu, Y. F., Y. Y. Xi, A. B. Djurisic and W. K. Chan (2008) ZnO nanorods for solar cells: Hydrothermal growth versus vapor deposition. *Applied Physics Letters*, 92, 133507-133509.
8. Kakiuchi, K., E. Hosono and S. Fujihara (2006) Enhanced photoelectrochemical performance of ZnO electrodes sensitized with N-719. *Journal of Photochemistry and Photobiology A: Chemistry*, 179, 81-86.
9. Keis, K., E. Magnusson, H. Lindstrom, S. E. Lindquist and A. Hagfeldt (2002) A 5% efficient photoelectrochemical solar cell based on nanostructured ZnO electrodes. *Solar Energy Materials and Solar Cells*, 73(1), 51-58.
10. Keis, K., L. Vayssieres, S. E. Lindquist and A. Hagfeldt (1999) Nanostructured ZnO electrodes for photovoltaic application. *Nanostructured Materials*, 12, 487-490.
11. Kong, Y. C., D. P. Yu, B. Zhang, W. Fang and S. Q. Feng (2001) Ultraviolet-emitting ZnO nanowires synthesized by a physical vapor deposition approach. *Applied Physics Letters*, 78, 407-409.
12. Lee, J. Y., Y. S. Choi, J. H. Kim, M. O. Park and S. Im (2002) Optimizing n-ZnO/p-Si heterojunctions for photodiode applications. *Thin Solid Films*, 403, 553-557.
13. Liang, S., H. Sheng, Y. Liu, Z. Hio, Y. Lu and H. Shen (2001) ZnO Schottky ultraviolet photodetectors. *Journal of Crystal Growth*, 225, 110-113.
14. Matsumura, M., S. Matsudaira, H. Tsubomura, M. Takata and H. Yanagida (1980) Dye sensitization and surface structures of semiconductor electrodes. *Industrial & Engineering Chemistry Product Research and Development*, 19(3), 415-421.
15. Pan, Z. W., Z. R. Dai and Z. L. Wang (2001) Nanobelts of semiconducting oxides. *Science*, 291, 1947-1949.
16. Park, W. I., D. H. Kim, S. W. Jung and G. Yi (2002) Metalorganic vapor-phase epitaxial growth of vertically well-aligned ZnO nanorods. *Applied Physics Letters*, 80, 4232-4234.
17. Redmond, G., D. Fitzmaurice and M. Graetzel (1994) Visible light sensitization by cis-Bis (thiocyanato) bis (2,2'-bipyridyl-4,4'-dicarboxylato) ruthenium (II) of a transparent nanocrystalline ZnO film prepared by sol-gel techniques. *Chemistry of Materials*, 6(5), 686-691.
18. Rensmo, H., K. Keis, H. Lindström, S. Södergren, A. Solbrand, A. Hagfeldt, S.-E. Lindquist, L. N. Wang and M. Muhammed (1997) High light-to-energy conversion efficiencies for solar cells based on nanostructured ZnO electrodes. *Journal of Physical Chemistry B*, 101(14), 2598-2601.
19. Tsubomura, H., M. Matsumura, Y. Nomura and T. Amamiya (1976) Dye sensitised zinc oxide: Aqueous electrolyte: Platinum photocell. *Nature*, 261, 402-403.
20. Vayssieres, L., K. Keis, A. Hagfeldt and S. E. Lindquist (2001) Three-dimensional array of highly oriented crystalline ZnO microtubes. *Chemistry of Materials*, 13,

4395-4398.

21. Vernardou, D., G. Kenanakis, S. Couris, A. C. Manikas, G. A. Voyiatzis, M. E. Pemble, E. Koudoumas and N. Katsarakis (2007) The effect of growth time on the morphology of ZnO structures deposited on Si (100) by the aqueous chemical growth technique. *Journal of Crystal Growth*, 308, 105-109.
22. Wang, J. and L. Gao (2004) Synthesis of uniform rod-like, multi-pod-like ZnO whiskers and their photoluminescence properties. *Journal of Crystal Growth*, 262, 290-294.
23. Wu, C. L., L. Chang, H. G. Chen, C. W. Lin, T. Chang, Y. C. Chao and J. K. Yan (2006) Growth and characterization of chemical-vapor-deposited zinc oxide nanorods. *Thin Solid Films*, 498, 137-141.
24. Yi, S. H., S. K. Choi, J. M. Jang, J. A. Kim and W. G. Jung (2007) Low-temperature growth of ZnO nanorods by chemical bath deposition. *Journal of Colloid and Interface Science*, 313, 705-710.

Received: Nov. 14, 2008 Revised: Dec. 19, 2008
Accepted: Feb. 20, 2009